

for this event. The shells collected for radiocarbon dating represent the presence of palaeo-river bank at that site. Subsequently, the river course was filled up with silt because of change in the river course. The sand dyke which is intruded into compact clay as well as the silt indicates that the sand dyke is younger than the river fill. Thus putting together the geological evidence of relatively compact dyke with upper bound of 1700 years and lower bounds of 5300 and 6000 years suggests an old seismic event during this time slot.

The event older than 25,000 years BP is inferred from upper bound sample (Figure 8, BH-10) age from Jayanagar site which is 26340 ± 2570 years BP. Lack of lower bound sample and considering the possibility of reworking of charcoal, one can expect the uncertainty in the age. However, the liquefaction feature observed at the site indicates an older seismic event.

Estimating the magnitude of a palaeoearthquake based on secondary features is still in the process of development. However, it is possible to make a semi-quantitative estimate based on liquefaction generated by the historical earthquakes. Two important parameters generally considered in this direction are thickness of sand dykes and farthest distance of liquefaction from the epicenter¹⁷. Though epicenter of palaeoearthquake is a critical component, it is not an easy task to locate it. Assuming that the epicenters of the historical earthquakes in this area^{10,11} are located in the Himalaya and our present observations show liquefaction features located at distances of 250–300 km away (Benibad, Muzaffarpur) from the assumed epicenters and utilizing the empirical relationship¹⁷, the approximate magnitude of the palaeoearthquakes turns out to be equivalent to that of large/great earthquake's magnitude.

From the above discussion, it is inferred that besides 1934 and 1833 events, at least two large/great events: one between 1700 and 5300 years BP and the other older than 25,000 years BP may have occurred in the North-Bihar and Nepal area, for which geological evidences could be traced out during the present study. Though we have been successful to a certain extent in identifying and dating a few palaeoseismic events in this seismically active area drained by shifting rivers, we must have missed some of the other older events due to lack of preservation of their signatures in this kind of environment. Thus by using palaeoliquefaction study, it is difficult to build up a complete record and recurrence interval for seismic events in such seismically active areas controlled by the phenomenon of shifting rivers.

4. Obermeier, S. F., USGS Prof. Paper 1336-B, 1989, pp. 1–114.
5. Tuttle, M. P. and Schweig, E. C., *Geology*, 1995, **23**, 253–256.
6. Wesnousky, S. G. and Leffler, L. M., *Bull. Seismol. Soc. Am.*, 1992, **82**, 1756–1785.
7. Talwani, P. and Schaeffer, J. *Geophys. Res.*, 2001, **106**, 6621–6642.
8. Sukhija, B. S., Rao, M. N., Reddy, D. V., Nagabhushanam, P., Hussain, S., Chadha, R. K. and Gupta, H. K., *Earth Planet. Sci. Lett.*, 1999a, **167**, 269–282.
9. Sukhija, B. S., Rao, M. N., Reddy, D. V., Nagabhushanam, P., Hussain, S., Chadha, R. K. and Gupta, H. K., *Tectonophysics*, 1999b, **308**, 53–65.
10. Bilham, R., *Curr. Sci.*, 1995, **69**, 101–128.
11. Pandey, M. R. and Molnar, P., *J. Nepal Geol. Soc.*, 1988, **5**, 23–45.
12. Dunn, J. A., Auden, J. B., Ghosh, A. M. N. and Roy, S. C., *Mem. Geol. Surv. India*, 1939 (reprinted 1981), **73**, 391.
13. Sinha, K. K. and Das Gupta, A. K., GSI Spl. Publ. no. 31, 1993, pp. 13–19.
14. Valdia, K. S., *Proc. Indian Natl. Sci. Acad.*, 1996, **A62**, 349–368.
15. Sinha, K. K. and Chatterjee, B., GSI Spl. Publ. no. 31, 1993, pp. 23–45.
16. Dasgupta, S., Mukhopadhyay, M. and Nandy, D. R., *Tectonophysics*, 1987, **136**, 255–264.
17. Obermeier, S. F., in *Paleoseismology* (ed. McCalpin, J. P.), Academic Press, London, 1996, pp. 331–396.

ACKNOWLEDGEMENTS. We thank Dr V. P. Dimri, Director, NGRI, Hyderabad for permission to publish the paper and Dr. H. K. Gupta, Secretary, Dept. of Ocean Development and former Director, NGRI for his keen interest in this work. The work was carried out with the financial support from Department of Science and Technology (DST), Government of India vide project no. DST/23(139)/ESS/97. We are grateful to Dr C. P. Rajendran and other two anonymous reviewers whose constructive criticism and suggestions have helped improve the manuscript.

Received 18 December 2001; revised accepted 12 August 2002

Gravity modelling across Satpura and Godavari Proterozoic Belts: Geophysical signatures of Proterozoic collision zones

D. C. Mishra*, B. Singh and S. B. Gupta

National Geophysical Research Institute, Hyderabad 500 007, India

The modelling of a gravity profile across the Satpura Fold Belt (SFB) constrained from seismic and other available information, suggests that the gravity high observed over the SFB is caused due to high-density upthrust blocks of lower crustal rocks in the upper crust exposed in some sections, and the gravity low towards the south of the Central Indian Shear (CIS) is caused due to low-density rocks below the Moho. The small-wavelength gravity lows and highs south of the CIS coincide with the felsic and the basic volcanics of tholeiitic to calc alkaline-type magmatism. These sig-

1. Bilham, R., Gaur, V. K. and Molnar, P., *Science*, 2001, **293**, 1442–1444.
2. McCalpin, J. P. (ed.), *Paleoseismology*, Academic Press, London, 1996, p. 583.
3. Yeats, R. S., Sieh, K. and Allen, C. R., *The Geology of Earthquakes*, Oxford University Press, New York, 1997, p. 568.

*For correspondence. (e-mail:

natures suggest that the SFB represents a Proterozoic collision zone between the Bundelkhand craton towards the north and the Bhandara craton towards the south, with the CIS as the suture and plausible subduction from the north to the south.

A 1000-km long NE–SW gravity profile across the Godavari Proterozoic Belt (GPB) and the Dharwar Craton (DC) also shows a regional gravity high over the GPB and a regional gravity low over the DC. They are interpreted due to high-density rocks in the upper crust and thickening of crust from 35 km under Eastern Dharwar Craton to 41 km under the Western Dharwar Craton respectively. These signatures along with contractional deformation of the Eastern and the Western GPB indicate that it represents a compressional terrane boundary between the Bhandara craton and the DC.

THERE is a growing consensus among the geoscientists in favour of the existence of plate tectonics during the Proterozoic period analogous to the present-day plate tectonics^{1,2}. The Indian peninsular shield, which consists of

several cratons (1–3, Figure 1) with Archean–Proterozoic assemblages of metasediments and metavolcanics, offers a unique opportunity to study the plausible signatures of plate tectonics during Proterozoic period. The Satpura Fold Belt (SFB) (5, Figure 1) is one of the major tectonic features in the central part of the Indian shield. It is bounded by the Central Indian Shear (CIS) (6, Figure 1) of early to middle Proterozoic period in the central part of its southern margin, and towards the north by the well-known Narmada–Son lineament (NSL) (4, Figure 1). The area south of the CIS is known as Bhandara craton (2, Figure 1), which is characterized by the Precambrian metavolcanics and metasediments representing the Sakoli, the Nandgaon, the Chilpi and the Khairagarh group of rocks of early to middle Proterozoic periods (2.4–1.6 Ga) (ref. 3). The volcanics are mainly tholeiitic in character, similar to the island arc tholeiitic–calcalkaline series³. The central part of the Bhandara craton is occupied by the Chhattisgarh basin (12, Figure 1), which contains metasediments of middle to late Proterozoic. It largely consists of thick piles of sandstone, shale,

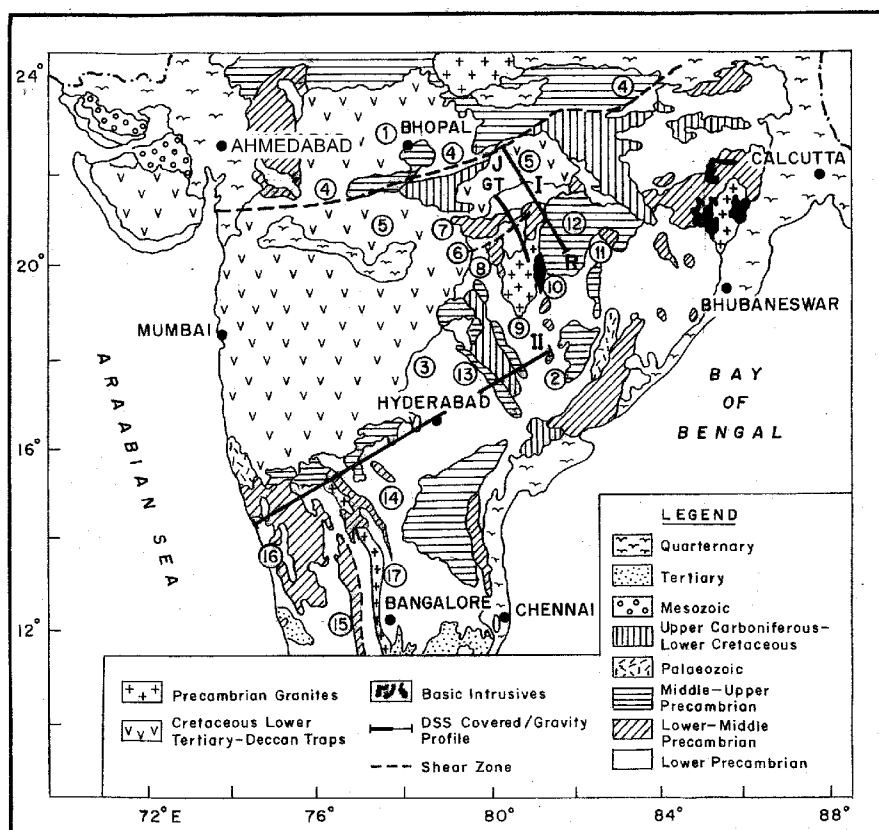


Figure 1. Geological map of central India⁴¹. Geological units discussed in the present study are marked by encircled numbers. 1, Bundelkhand craton; 2, Bhandara craton; 3, Dharwar craton; 4, Narmada Son Lineament; 5, Satpura Fold Belt; 6, Central Indian Shear; 7, Sausar group; 8, Sakoli group; 9, Dongargarh granitoid; 10, Basic Volcanics; 11, Sonakhan Schist Belt; 12, Chhattisgarh basin; 13, Godavari Proterozoic Belt; 14, Eastern Dharwar Craton; 15, Shear Zone; 16, Western Dharwar Craton and 17, Closepet granite. A geotranssect (GT) across the SFB and profiles I and II, are also shown. Profile I extends from Jabalpur (J) to Raipur (R).

limestone and volcanic ash of shallow marine condition⁴. The basement for the Chhattisgarh basin is formed by the Sonakhan Schist Belt (11, Figure 1) of late Archean to early Proterozoic period⁵, which is exposed towards the south of this basin and consists of volcano sedimentary sequences with bimodal volcanics of presumably back-arc setting. There are also large granitic plutons in the Bhandara craton such as Dongargarh (9, Figure 1) and the Malanjhand granitoid of early–middle Proterozoic period (1.8 Ga), which have intruded the Amgaon gneisses and show a N–S foliation trend. The region just north of the CIS is characterized by high- to intermediate-grade Sausar group of rocks (7, Figure 1) of late Archean–early Proterozoic period oriented parallel to the CIS (NE–SW), and includes patches of exposed granulite rocks along the CIS. There is a distinct separation of low- and high-grade rocks towards the south and the north of the CIS respectively, and island arc-type magmatism south of it. These signatures have been interpreted, as the result of Proterozoic collision with subduction from the north to the south³.

The Godavari Proterozoic Belt (GPB) of middle to late Proterozoic period (1.3–0.87 Ga) (ref. 6) is exposed south of the Bhandara craton, and is oriented (NW–SE) in a direction different from the general structural trend of the Bhandara craton (N–S) (Figure 1). The GPB is exposed in two linear zones along the eastern and the western side of the exposed Gondwana sediments. The two belts largely consist of sandstone, shale, limestone and quartzite and are deposited under different marine conditions, from shallow continental shelf to deep basins, and are largely devoid of volcanic rocks⁷. There are distinct differences in the nature of sediments comprising the eastern and the western GPB⁷, with contractional deformation in them. The basement consists of gneisses with lower crustal granulite rocks reported from specific sections whose metamorphic age is 2.55 Ga (ref. 8). The Gondwana sediments overlying the GPB belong to Permian–Triassic times and are represented by sandstone, shale, limestone, etc. deposited in a rift basin⁹. The Dharwar craton (DC) (3, Figure 1) is located to the south of Bundelkhand and Bhandara cratons, and is covered by basalt of Deccan Volcanic Province (DVP) towards the northwest (5, Figure 1). The southern part of the DC is characterized by Dharwar supergroup of rocks representing Dharwar Schist Belt (DSB) and granitic plutons of late Archean to early Proterozoic periods¹⁰. They were considered part of early Proterozoic mobile belt¹¹. The DC is divided into the Eastern and the Western cratons (14, 16, Figure 1) separated by a shear zone (15, Figure 1) characterized by intense shearing and associated mylonites¹².

Based on gravity¹³ and Deep Seismic Sounding (DSS)¹⁴ studies, SFB has been interpreted as a horst. The reflectivity pattern across the CIS along a geotranssect (GT, Figure 1), 100–150 km west of profile I, depicts opposite dipping reflectors and a hump in the upper crust

under the SFB¹⁵. Magnetotelluric studies¹⁶ along the same geotranssect indicate different conductivity distribution on either side of the CIS, with high conductivity rocks in the upper crust under the SFB north of the CIS. A bipolar gravity anomaly¹⁷ with gravity high coinciding with the lower crustal rocks under the SFB and gravity low south of it, was observed along this GT. Such bipolar gravity anomalies supported from other evidences have been related to Proterozoic collision zones in other parts of the world^{18,19}. A DSS profile across the Godavari basin indicates a high-velocity layer at a shallow depth of 5–6 km, and a thick crust of 41–42 km (ref. 20). The gravity modelling across the GPB suggests high-density basement rocks representing lower crustal rocks²¹ exposed in some sections. Eastern Dharwar craton (EDC) is characterized by normal crustal thickness of 34–35 km and felsic to intermediate composition of the lower crust^{22,23}, implying lower seismic velocities in the lower crust. However, the Western Dharwar craton (WDC) has 40–42-km thick crust^{24,25}, with lower seismic velocities in the crust and the upper mantle^{26,27}. Keeping the above facts in mind, we have carried out gravity modelling along profiles I and II, to derive the crust and upper mantle structure and understand the various tectonic and geodynamic processes across these terranes.

For the gravity profile across the SFB (profile 1, Figure 1), gravity observations along Jabalpur to Raipur are recorded along the road at 1 km station interval using Lacoste and Romberg gravimeter. The elevation of each gravity station is recorded using an altimeter, which is connected to the benchmarks of Survey of India. The reduced elevation has an accuracy of about 3–5 m, resulting in an accuracy of better than 2 mGal in the final Bouguer anomaly computations. Figure 2 shows free-air anomaly, Bouguer anomaly, elevation and exposed geology along this profile. The elevated topography in the centre (Figure 2a) corresponds to Satpura mountain ranges. The free-air and Bouguer anomalies show positive correlation with elevation, indicating lack of isostatic compensation. The gravity ‘highs’ over the elevated topography in such cases usually suggest the presence of anomalous subsurface high-density rocks. The Bouguer anomaly (Figure 2c) shows a bipolar regional gravity anomaly with a gravity high over the SFB and a large wavelength gravity low over the adjoining Bhandara craton.

An unbiased estimate of isostatic regional anomaly is obtained using the zero free-air values (Figure 2) which indicate isostatic equilibrium²⁸. The zero free-air anomaly over a plateau usually indicates that the gravity effect of topographic load above the mean sea level is balanced due to crustal thickening. The plot of zero free-air in the present case (Figure 2c) shows step-like anomaly, which indicates low-density rocks along the Moho towards the southern part. The step-like anomaly indicates contact separating blocks of different densities. The isostatic regional anomaly has therefore been modelled due to a

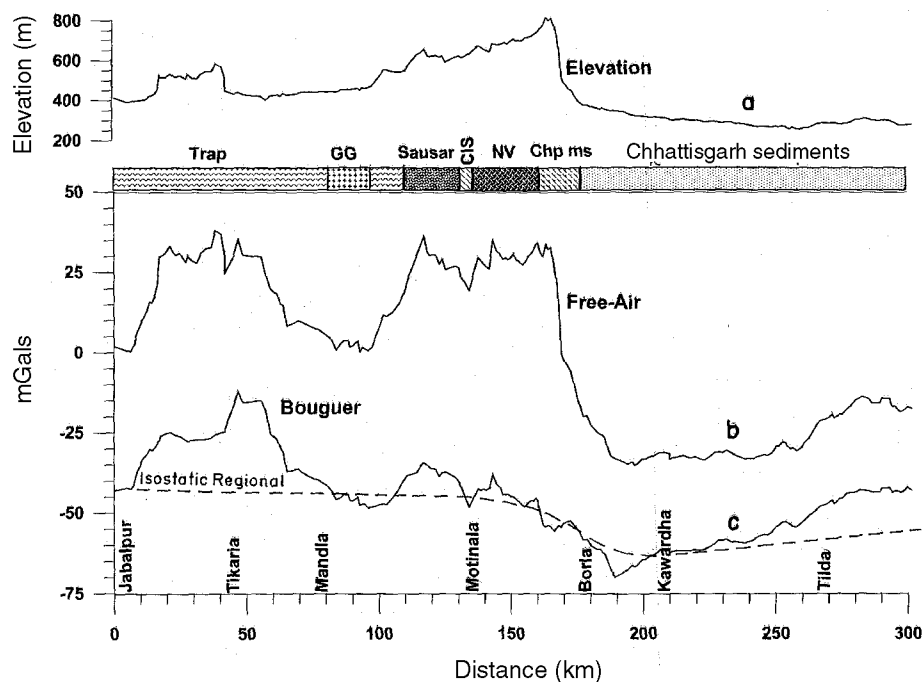


Figure 2. Observed elevation, free-air and Bouguer anomalies along profile I. Isostatic regional anomaly curve is obtained by joining those Bouguer anomaly values for which free-air anomaly is zero. (Top) Exposed geology. GG, Granite gneiss; NV, Nandgaon volcanics; Chp ms, Chilpi group of metasediments, and CIS, Central Indian Shear.

combination of (i) blocks of different densities in the lower crust with a higher bulk density (2.86 g/cm^3) towards the north (2, Figure 3) compared to the lower bulk density (2.83 g/cm^3) towards the south (3, Figure 3), and (ii) a low-density (2.98 g/cm^3) dipping block below the Moho in the south (5, Figure 3). These causative sources are constrained from the results of seismic and magnetotelluric investigations along the geotransect (GT; Figure 1) west of this profile, as discussed above. The contact of lower crustal blocks, when projected on the surface, coincides approximately with the CIS. The shallow sources are controlled from the exposed geology. The gravity anomaly at the northern end of the profile, south of Jabalpur can be decomposed into three components B, C and D. Anomaly B is modelled due to a high-density body in the upper crust (6, Figure 3) which corroborates with the structure derived from the seismic and MT studies along the geotransect. However, the components C and D are caused by shallow, high-density bodies (8 and 9, Figure 3), which corroborates with shallow seismic tomography and also from the results of resistivity sounding, south of Jabalpur^{29,30}. They may represent Mahakoschal group of rocks extending under the exposed Deccan trap in this section (8, Figure 3) and an intrusive body similar to body 6 (9, Figure 3) respectively. The top layer in this region (7, Figure 3) represents Deccan trap of a few hundred metres thickness. The other shallow sources numbered as 9–14 (Figure 3), are based on the exposed rock types. The CIS (11, Figure 4) itself is characterized by a small gravity 'low' similar to

the signature of the CIS along the adjacent geo-transect¹⁷ and is modelled due to a low-density body which may represent a fractured zone. The gravity high north of the CIS is caused by Sausar metasediments and the lower crustal granulite rocks (10, Figure 3) exposed along the CIS. The gravity 'high' and 'lows' south of the CIS represent Nandgaon volcanics and Chilpi group of metasediments (12 and 13, Figure 3). The gravity low and high in the southern part of the profile are attributed to low- and high-density bodies (15 and 16, Figure 3) in the basement below Chhattisgarh basin (14, Figure 3), which may represent a granite intrusive body, as several such bodies are exposed in this region and the extension of the Sonakhan schist belt exposed south of Chhattisgarh sediments (11, Figure 1).

The gravity profile across the GPB and DC (profile II, Figure 1) is a 1000-km long profile (Figure 4) starting from the west coast of India, traversing through Hyderabad across the DC and the GPB. The gravity data along this profile are obtained from the Bouguer anomaly map of India³¹. The large gravity 'low' (A) over the Godavari basin is modelled by the exposed Gondwana sediments³², while flanking gravity highs (B and C) are caused by high-density rocks representing lower crustal rocks²¹. Thus, if the gravity effect of the low-density Gondwana sediments is removed, the gravity anomaly will be as shown by a dotted line in Figure 4. This anomaly coincides with a fifth-order polynomial surface representing the regional field along this profile. This regional anomaly shows gravity high towards the north and a large-

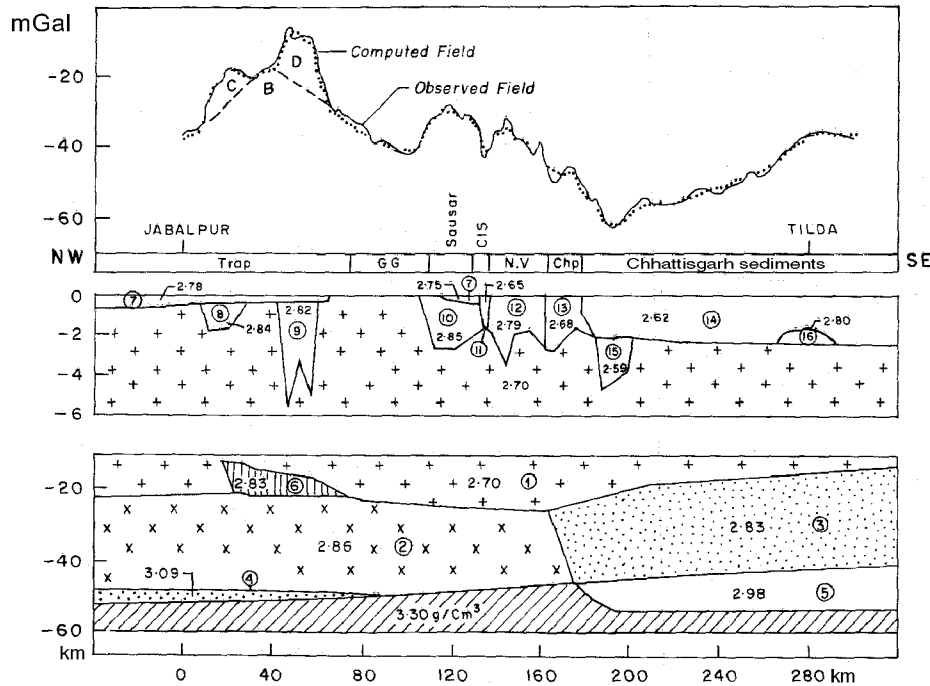


Figure 3. Observed and computed Bouguer anomaly along profile I with the modelled crustal section. Bodies are numbered 1–16 with their densities shown in g/cm^3 .

wavelength gravity low towards the south, forming a bipolar anomaly. The regional gravity anomalies are modelled using constraints from DSS and tomographic results. The presence of high seismic velocities in the upper–middle crust under the GPB provides initial constraints for the existence of high-density body (1, Figure 4) to explain the gravity high over the GPB. Similarly, thickening of crust (2, Figure 4) by about 6 km under the WDC with respect to a normal crustal thickness of 35 km under the EDC near Hyderabad^{22,24,25} provided an initial model to explain the regional gravity low observed over the WDC. It is interesting to note that for a thick crust of 41–42 km, the estimated density contrast of -0.12 g/cm^3 for the thickened part of the crust is much less than the normal density contrast of -0.4 g/cm^3 between the lower crust (2.9 g/cm^3) and the upper mantle (3.3 g/cm^3), indicating that either the density of the causative body is higher than that of the normal density of the lower crust, or the density of the upper mantle is less compared to its normal density or both. The short-wavelength gravity lows and highs at the southern end of this profile (D–F, Figure 4) across the DC can be qualitatively attributed to low- and high-density rocks of the schist belts.

Geophysical signatures over the recent collision plate boundaries are distinct and well understood^{33,34}. However, existence of plate tectonic process during the Proterozoic period is not well understood and remains largely unresolved. But recent deep seismic experiments carried out over ancient terranes show some characteristic signature indicative of the existence of present-day plate tectonic processes during Archean–Proterozoic

times^{35,36}. A gravity profile across the SFB shows a bipolar gravity anomaly. The crustal density model across the SFB indicates a high-density body in the upper crust beneath the SFB (6, Figure 3), which represents an upthrust block of lower crustal granulite rocks. The presence of high seismic velocity at shallow depth under the SFB^{15,37} supports the above conclusion. It is also supported by the presence of a conductive body almost at the same depth along a geotranssect west of this profile¹⁶. The low-density body (5, Figure 3) below the Moho in the southeast coincides with the dipping reflectors of low velocity³⁸ in the upper mantle along the adjoining geotranssect (GT, Figure 1). Dipping reflectors below the Moho are indicative of subducted crustal rocks in other parts of the world³⁶. There is a bipolar, regional gravity anomaly with the gravity high coinciding with the younger province of the SFB and the gravity low coinciding with the older Bhandara craton. The former shows a larger crustal thickness than the latter, with low-density rocks in the upper mantle indicating a collision zone¹⁹. The maximum gradient of gravity anomaly over younger and older provinces is 0.5 and 0.2 mGal km^{-1} , which is within the range suggested for Proterozoic collision zones in the Candian shield¹⁹. These considerations, along with the occurrences of tholeiitic- to calcalkaline-type of basic and felsic volcanics and back-arc rift settings in the Bhandara craton are consistent with the low-density body below the Moho, which may represent the remnants of subducted crustal rocks. Bodies 8 and 9 (Figure 3) towards the NW represent the extension of Mahakoschal group of rocks, which are exposed north of

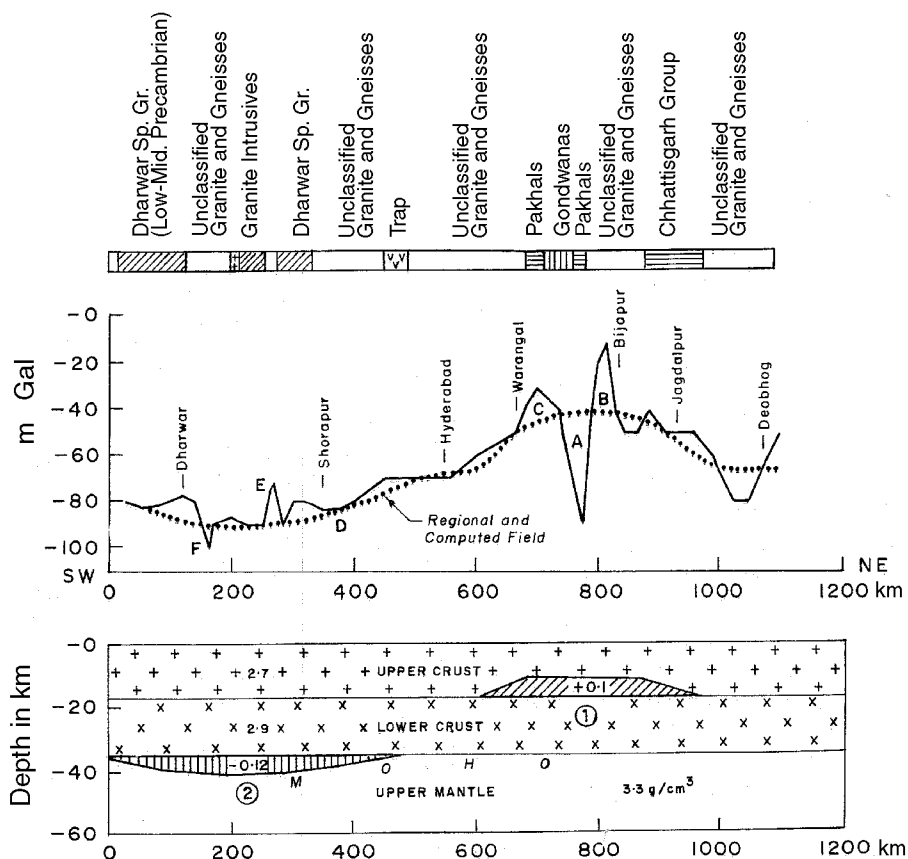


Figure 4. Gravity profile II and computed regional field due to bodies with their density contrast in g/cm^3 . Body 1 represents high-density rocks under the GPB, and body 2 represents the low-density body along the Moho, indicating a thick crust under the WDC. (Top) Exposed geology.

this area and a high-density body in the basement which may be similar to body 6 representing lower crustal rocks supported from high-velocity at a shallow depth³⁷. Body 10 (Figure 3) represents the intermediate-grade Sausar metasediments and high-grade lower crustal rocks, which are exposed in certain sections north of the CIS. The CIS (11, Figure 3) is represented by a low-density body, which may represent saturated fractured rocks, as indicated by low-density and high conductive rocks under the CIS along the geotranssect, west of this profile. Occurrences of the Nandgaon volcanics of early Proterozoic period (2.4 Ga) and Chilpi group of metavolcanics of middle Proterozoic (1.6 Ga) and metasediments (12 and 13, Figure 3) south of the CIS represent tholeiitic to calc alkaline, island arc-type magmatism in back-arc rift type basins³. The low and high-density bodies (15 and 16, Figure 3) below Chhattisgarh sediments (14, Figure 3) may represent granitic intrusion in the basement, as several granitic plutons are exposed in this area and extension of Sonkhan schist belt, which are exposed towards the south. The granitic plutons of Bhandara craton such as Dongargarh pluton (9, Figure 1) of early-middle Proterozoic period (1.8 Ga) are K-granite plutons showing island-arc affinity. From the density model and rock types discussed above, it is apparent that the two blocks

towards the north and the south of the CIS are different, which collided during early Proterozoic period and the SFB and the CIS represent respectively, the collision zone and the suture between the two blocks. The low-density body below the Moho, south of the CIS and island-arc and back-arc type magmatism in this section suggest plausible subduction from the north to the south. The extension of linear gravity high all along the SFB³⁰ suggests the extension of upthrust, lower crustal rocks all along the SFB. It suggests, therefore, that the entire section of the SFB might have been involved in the collision between the Bundelkhand craton toward the north and the DC and Bhandara craton towards the south. The Sausar basin of late Archean-early Proterozoic period along the southern margin of the SFB with deformed marine sediments, may represent a peripheral foreland basin. These sediments of late Archean-early Proterozoic and Sonakhan schist belt of Bhandara craton consisting of contemporary volcano sedimentary sequences representing back-arc rift basin, indicate that subduction across the CIS might have started earlier during late Archean period. This process continued intermittently up to middle Proterozoic, as indicated by K-granite plutons of this period in the form of Dongargarh and Malanjhand granitoids and other rock types such as Chilpi group of rocks, Kairagarh volcanics, etc.

A gravity profile across the GPB and the DC also shows a bipolar regional gravity anomaly, where the gravity high coincides with the high-density, exhumed lower crustal rocks along and under the GPB and large-wavelength gravity low coincides with the exposed low-grade gneisses/granite of the DC. The modelling of this regional gravity anomaly constrained from seismic information suggests a high-density body in the upper crust under the GPB, north of Hyderabad and a low-density body along the Moho under the WDC, southwest of Hyderabad. The high-density body under the GPB also shows high seismic velocity and may represent up-thrusted, lower crustal rocks which are exposed in some sections⁸. The low-density body at the base of the crust under the WDC, southwest of Hyderabad represents thickening of the crust. The low-density rock at Moho (2, Figure 4) with a maximum plausible density contrast of -0.12 g/cm^3 provides a density estimate of 3.18 g/cm^3 for this body, if the normal upper mantle density is taken as 3.3 g/cm^3 . This suggest that this body is mafic in nature and may represent an underplated crust. An underplated crust and low-velocity/low-density upper mantle north of this area have been suggested based on seismic studies and gravity modelling^{39,40}, which indicated a maximum density of 3.1 g/cm^3 for the underplated part, usually the maximum density assigned to underplated crust. Therefore, presuming that the density of the underplated part of the crust in this section is also 3.1 g/cm^3 , the density of the upper mantle under the WDC will be 3.22 g/cm^3 , which is almost the same as that reported north of this area³⁹, and is lower than the normal density of the upper mantle (3.3 g/cm^3). This indicates a low-density upper mantle under the WDC, which is synonymous with the low velocity, as discussed above²³. The gravity high of the bipolar gravity anomaly coinciding with the younger province of the GPB and its low coinciding with the older province of the DC again indicate a zone of compression¹⁹. The high-density and high-velocity rocks under the GPB, the contractional deformation in the sediments of the eastern GPB and differences in the sediment of the eastern and the western GPB further suggest that it represents a compressional tectonics. It is supported from low-velocity and low-density rocks in the upper mantle under the WDC. The shelf type of metasediments of middle-late Proterozoic period along the GPB may represent peripheral foreland basins.

1. Koerner, A., *Tectonophysics*, 1991, **187**, 393–410.
2. Windley, B. F., *The Evolving Continents*, Wiley, 1995, 3rd edn.
3. Yedekar, D. B., Jain, S. C., Nair, K. K. K. and Dutta, K. K., *Spec. Publ., Geol. Surv. India*, 1990, **28**, 1–43.
4. Murti, K. S., *Mem. Geol. Soc. India*, 1987, **6**, 239–260.
5. Das, N., Royburman, K. J., Vatsa, U. S. and Mahurkar, Y. V., *Spec. Publ., Geol. Surv. India*, 1990, **28**, 118–132.
6. Chaudhuri, A. K., Mukhopadhyay, J., Patranibis Deb, S. and Chanda, S. K., *Gondwana Res.*, 1998, **2**, 213–225.

7. Sreenivasa Rao, T., Proceedings of the Ninth International Gondwana Symposium, Hyderabad, 1994, pp. 855–877.
8. Rajesham, T., Bhasker Rao, V. J. and Murthy, K. S., *J. Geol. Soc. India*, 1993, **41**, 51–59.
9. Raja Rao, C. S., *Geol. Surv. India Bull.*, 1982, **45**, 1–103.
10. Naqvi, S. M. and Rogers, John J. W., *Precambrian Geology of India*, Oxford University Press, 1987, pp. 1–223.
11. Radhakrishna, B. P. and Naqvi, S. M., *J. Geol.*, 1986, **92**, 145–166.
12. Drury, S. A. and Holt, R. W., *Tectonophysics*, 1980, **65**, 1–15.
13. Qureshy, M. N. and Warsi, W. E. K., *R. Astron. Soc. Geophys. J.*, 1980, **61**, 235–242.
14. Kaila, K. L., Reddy, P. R., Dixit, M. M. and Koteswar Rao, P., *J. Geol. Soc. India*, 1985, **26**, 468–485.
15. Reddy, P. R. *et al.*, *Mem. Geol. Soc. India*, 1995, **31**, 537–544.
16. Sarma, S. V. S. *et al.*, Proceedings of the International Seminar of Association of Expl. Geophysicists, Hyderabad, 1996, pp. 206–207.
17. Mishra, D. C., Singh, B., Tiwari, V. M., Gupta, S. B. and Rao, M. B. S. V., *Precambrian Res.*, 2000, **99**, 149–169.
18. Fountain, D. M. and Salisbury, M. H., *Earth Planet. Sci. Lett.*, 1981, **56**, 263–277.
19. Gibb, R. A. and Thomas, M. D., *Nature*, 1976, **262**, 199–200.
20. Kaila, K. L., Murthy, P. R. K., Rao, V. K. and Venkateswarlu, N., *Tectonophysics*, 1990, **173**, 307–317.
21. Mishra, D. C., Chandrasekhar, D. V., Venkata Raju, D. Ch. and Vijaya Kumar, V., *Earth Planet. Sci. Lett.*, 1999, **172**, 287–300.
22. Saul, J., Ravi Kumar, M. and Sarkar, D., *Geophys. Res. Lett.*, 2000 (in press).
23. Mishra, D. C., *Gondwana Res.*, 2002 (commun.)
24. Reddy, P. R., Chandrakala, K. and Sridhar, A. R., *J. Geol. Soc. India*, 2000.
25. Kaila, K. L. *et al.*, *ibid*, 1979, **20**, 307–333.
26. Srinagesh, D. and Rai, S. S., *Phys. Earth Planet. Inter.*, 1996, **97**, 27–41.
27. Rai, S. S., personal commun., 2002.
28. Subba Rao, D. V., *Geophys. Res. Lett.*, 1996, **23**, 3543–3546.
29. Rao, K. V., Srirama, B. V. and Ramasastry, P., *Spec. Publ., Geol. Surv. India*, 1990, 99–117.
30. Reddy, P. R., Sain, K. and Murthy, A. S. N., *Curr. Sci.*, 1997, **73**, 796–800.
31. Report, National Geophysical Research Institute, Hyderabad, 1975.
32. Mishra, D. C., Gupta, S. B. and Venkatrayudu, M., *Earth Planet. Sci. Lett.*, 1989, **94**, 344–352.
33. Holiger, K. and Kissling, E., *Geophys. J. Int.*, 1992, **3**, 213–225.
34. Jin, Y., McNutt, M. K. and Zhu, Y. S., *J. Geophys. Res.*, 1996, **11**, 275–290.
35. Riahi, M. A. and Lund, C. E., *Tectonophysics*, 1994, **239**, 149–164.
36. Mooney, W. D. and Meissner, R., *Continental Lower Crust*, Elsevier Science, The Netherlands, 1992, pp. 45–79.
37. Prakash Kumar and Tewari, H. C., *Geophys. J. Int.*, 2000 (in press).
38. Reddy, P. R. and Satyavani, N., *Curr. Sci.*, 2001, **80**, 685–687.
39. Tiwari, V. M., Vyaghreswara Rao, M. B. S. and Mishra, D. C., *J. Geodyn.*, 2001, **31**, 1–17.
40. Kennet, B. L. N. and Widiyantoro, *Earth Planet. Sci. Lett.*, 1999, **165**, 145–155.
41. Geological Map of India, Geological Survey of India, Kolkata, 1993.

ACKNOWLEDGEMENTS. We thank the Director, National Geographical Research Institute, Hyderabad for his support and permission to publish this work. We also thank the anonymous reviewer for his constructive suggestions.

Received 11 April 2002; revised accepted 5 September 2002